Int. J. Solids Structures Vol. 18, No. 7, pp. 619–641, 1982
Printed in Great Britain.

0020-7683/82/070619-23$03.00/0

EXPERIMENTAL AND THEORETICAL STUDIES OF COLUMNS UNDER AXIAL IMPACT†

J. ARI-GUR, T. WELLER and J. SINGER

Department of Aeronautical Engineering, Technion-Israel Institute of Technology, Haifa, Israel

(*Received* 24 *November* 1980; *in revised form* 20 *March* 1981)

Abstract—The dynamic response of columns loaded by an impulsive axial compression was studied experimentally and theoretically. Approximate criteria for determination of dynamic buckling are discussed and applied. The investigation was carried out on clamped specimens, made of metals and composite materials, loaded impulsively by a striking mass. In the theoretical study Rayleigh-type beam equations are assumed for a geometrically imperfect column of a linear-elastic anisotropic material. A numerical solution, by a finite-difference approach, yields buckling behavior which correlates well with the experimental results. It is shown that initial geometrical imperfection, duration of impulse and effective slenderness have a major influence on the buckling loads whereas the effect of the material is secondary. The major effects are presented in a form that can guide the designer.

NOTATION

- A elastic modulus, eqn (3.5)
- B coupling modulus, eqn (3.5)
- b width of cross-section of column
- C_L, C_T damping coefficients, eqn (3.28)
- c velocity of propagation of longitudinal wave, eqn (3.10)
- D bending modulus, eqn (3.5)
- DLF Dynamic Amplification Load Factor, eqn (2.3)
- E modulus of elasticity
- h thickness of column
- L length of column
- M striking mass
- M_0 intermediate mass
- M_x moment per unit length, eqn (3.3)
- m mass of column
- N_x force per unit length, eqn (3.3)
- R_L, R_T damping coefficients, eqns (3.28)
- r radius of gyration = $\sqrt{\left(\frac{D}{A}-\frac{B^2}{A^2}\right)}$
- r_0 "symmetric" radius of gyration, eqn (3.11)
- T duration of impulse
- t time
- U axial displacement of striking mass
- u axial displacement
- V velocity of striking mass
- V_0 striking velocity
- w deflection from axis, Fig. 8
- w_0 initial geometrical imperfection
- x axial coordinate, Fig. 8
- z transverse coordinate, Fig. 8
- α coefficient, eqn (3.33)
- β coefficient, eqn (3.33)
- Δt, Δx differences
- Δw deflection = $w - w_0$
- ϵ strain
- ζ normal coordinate, Fig. 8
- κ curvature
- λ slenderness of column, eqns (2.1), (3.12)
- ρ mass density
- σ stress
- τ non-dimensional duration of impulse, eqn (2.4)
- $(\,)_b$ bending
- $(\,)_c$ compression
- $(\,)_{cr}$ critical

†The paper was presented at the IUTAM 15th Int. Congress of Theoretical and Applied Mechanics, Toronto, August 1980. Part of the research was carried out in cooperation with Dornier GmbH.

$( )_d$ dynamic
$( )_E$ Euler
$( )_{eff}$ effective
$( )_{max}$ maximum
$\bar{( )}$ nondimensional parameter
$( )_{,}$ partial differentiation
$( )'$ nondimensional spatial derivative
$\dot{( )}$ nondimensional time derivative

1. INTRODUCTION

Many engineers are confronted with the problem of "dynamic buckling" or "dynamic instability" of structures subjected to an impulsive compression. A column, too, may lose stability when loaded by a compressive force of short duration. One of the earliest studies on this subject is that of Koning and Taub[1]. They treated a column loaded by a constant axial compression for a specified period of time and showed that when the axial load is greater than the static buckling load the deflection increases exponentially with time. Meier[2] showed that a column subjected to a rapidly applied axial stress may withstand compressive loads much in excess of the static buckling loads. These high buckling loads are confined to short durations of loading. The studies of[1, 2], like other investigations (see, e.g. [3, 4, 10]) assumed that the initial geometrical imperfection and the resulting deflection have the shape of a half sine wave and that effects of axial inertia may be ignored. The neglect of axial inertia terms may be permissible for low rates of loading, like those occurring, e.g. in universal loading machines. This problem was studied by Hoff[4] and some other investigators[5–7], and was extended by Sevin[8] to include axial inertia.

For loadings of short duration wave propagation phenomena become important. A customary manner of impulsive loading is by a collision with a striking mass (M). The analysis for the propagating stress field developed after axial impact is given in texts like[9]. Hayashi and Sano[10, 11] investigated the response of a column with initial geometrical imperfection impacted axially with a striking mass. In[11] they included axial inertia terms in their analysis, compared several beam theories and presented some test results. Their study appears to be incomplete, in particular from an engineering point of view, because they did not attempt to define dynamic buckling loads. In[12, 13] more extensive literature surveys have been carried out, but no presentation of design information for prediction of the "dynamic buckling" load for a given column and loading has been found.

The aim of the present investigation is therefore to define suitable criteria for determination of dynamic buckling loads, to identify the dominant parameters of the phenomenon, to consider their effects and to provide useful information and charts for the designer. The study includes both analysis and experiments and most of the conclusions are verified by both methods.

2. EXPERIMENTS

Test set-up and procedure

An impulsive axial compression of a column is produced by direct collision with a striking mass. A special test rig (see Fig. 1) was designed and built in order to attain controlled speed and direction of the striking mass at collision and repeatability of the response of the impacted column.

The test rig includes a vertical tube along which a cylindrical mass can be dropped from any desired height to strike a specimen positioned under the tube. With the aid of an accelerating spring, velocities of up to 15 m/sec were obtained. Various striking masses may be employed to achieve desired durations of impulse. Since rebound is not prevented, the impulse transferred to the column is larger than the momentum of the striking mass. Second impact is not prevented, but it is weaker and occurs after the maximum deflection is obtained.

The specimens are of thin rectangular cross-section. The lower edge of the column is clamped by a massive grip resting on the ground. The upper edge is inserted into a cylinder made of Akulon (tradename for type 6 Nylon) which serves as a light-weight slide bearing inside the

Fig. 1. Test set up for dynamic buckling.

vertical tube. The motion of the impacted edge is therefore restrained to the axial direction only and the boundary conditions approximate clamped-clamped conditions.

The response of a column in a typical impact test is measured by a pair of strain gages, located at the middle of the column length. The response of each gage is recorded separately by a Biomation model 805 waveform high frequency digital recorder. These records are then plotted (see Fig. 2) simultaneously with their summation and subtraction results, to yield records of the compression and bending responses, respectively. In a test, a specimen is impacted with increasing velocities, and these responses are plotted for each impact.

Test results

Results for 15 steel specimens ("Wardson" ground flat oil hardening AISI–01 carbon chrome alloy in untempered condition) and 17 aluminum alloy specimens (6061–T4) are presented in Tables 1 and 2, respectively. The effective slenderness is defined by

$$\lambda_{\text{eff}} = \frac{L_{\text{eff}}}{r} \tag{2.1}$$

where $L_{\text{eff}} = \frac{L}{2}$ for clamped boundaries and $r = h/\sqrt{12}$ is the radius of gyration of the rectangular cross-section of the isotropic columns. The static buckling strain is calculated by the Euler equation

$$\epsilon_{cr_E} = \left(\frac{\pi}{\lambda_{\text{eff}}}\right)^2. \tag{2.2}$$

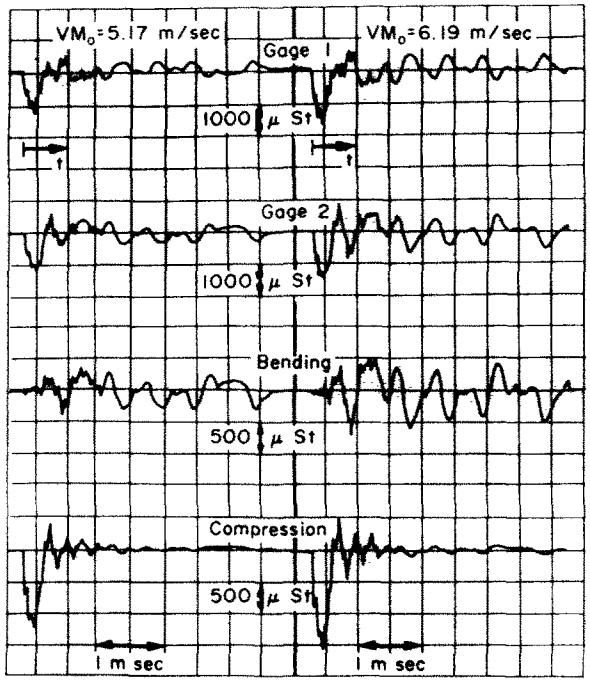

Fig. 2. Typical strain records of two separate impact tests on a column.

Typical plots of the maximum flexural response (ϵ_b) vs the peak magnitude of the impulsive compression (ϵ_c) are presented in Figs. 3(a) and (b), where each point corresponds to one impact test. In this presentation of the over-all behavior of a column two separate regions are observed; in the first region the slope of the curve is quite moderate, while in the second region a small increase in the dynamic compression results in a much larger increase in the bending

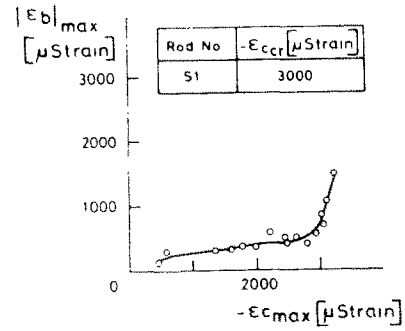

a STEEL

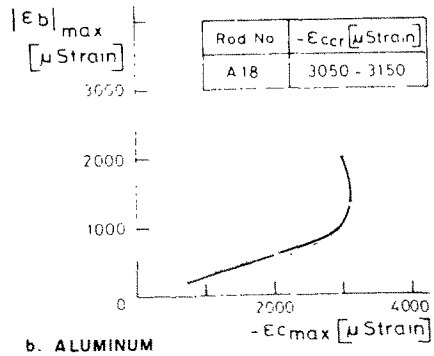

b. ALUMINUM

Fig. 3. Typical bending-compression plots of metal columns

Table 1. Clamped steel columns under direct axial impact

Specimen No.	L Length [mm]	b Width [mm]	h Thickness [mm]	λ_{eff} Effective slenderness	ϵ_{Cr_E} Euler buckling strain [μ strain]	ϵ_{Cr_n} Dynamic buckling strain [μ strain]	DLF Dynamic load factor	m Mass [gr]	M Striking mass [gr]	$\frac{\pi}{2}\sqrt{\frac{M}{m}}$	V_{CT} Critical striking velocity [m/sec]
1	2	3	4	5	6	7	8	9	10	11	12
Y1	270	19.05	1.6	292	116	2550	22.0	75	180	2.4	7.86
Y2	110	19.05	1.6	119	696	2700	3.9	36	180	3.5	6.11
Y3	190	19.05	1.6	206	233	3350	14.4	53	180	2.9	8.86
Y4	150	19.05	1.6	162	374	3725	10.0	44	180	3.2	9.61
Y5	230	19.05	1.6	249	159	3350	21.1	63	180	2.7	10.05
Y6	90	19.05	1.6	97	1040	3825	3.7	31	180	3.8	8.77
S1	190	19.05	3.2	103	930	3000	3.2	108	370	2.9	8.35
S2	190	19.05	3.2	103	930	2800	3.0	108	370	2.9	8.97
S3	190	19.05	1.6	206	233	3250	13.9	53	180	2.9	9.17
S4	190	19.05	2.4	137	525	3000	5.7	81	275	2.9	8.91
S5	190	19.05	2.4	137	525	3000	5.7	81	275	2.9	9.18
S6	190	19.05	0.8	411	58	1350	23.3	28	95	2.9	5.63
S7	190	19.05	0.8	411	58	1400	24.1	28	95	2.9	5.27
YS1	380	19.05	1.6	411	58	1775	30.6	99	332	2.9	5.10
YS2	380	19.05	1.6	411	58	1800	31.0	99	332	2.9	5.63

Table 2. Clamped aluminium alloy columns under direct axial impact

Specimen No.	L Length [mm]	b Width [mm]	h Thickness [mm]	λ_{eff} Effective slenderness	ϵ_{Cr_E} Euler buckling strain [μstrain]	ϵ_{Cr_D} Dynamic buckling strain [μstrain]	DLF Dynamic load factor	m Mass [gr]	M Striking mass [gr]	$\frac{\pi}{2}\sqrt{\frac{M}{m}}$	V_{CT} Critical striking velocity [m/sec]
1	2	3	4	5	6	7	8	9	10	11	12
A1	270	19.05	1.6	292	116	3550	30.6	25	63	2.5	14.39
A2	90	19.05	1.6	97	1040	4050	3.9	11	63	3.8	10.03
A3	110	19.05	1.6	119	696	3500	5.0	12	63	3.6	8.81
A4	150	19.05	1.6	162	374	3650	9.8	15	63	3.2	9.97
A5	190	19.05	1.6	206	233	4200	18.0	19	63	2.9	9.80
A6	230	19.05	1.6	249	159	3050	19.2	22	63	2.7	10.77
A7	230	19.05	1.6	249	159	2400	15.1	21.5	63	2.7	8.15
A8	270	19.05	1.6	292	116	2700	23.3	25	63	2.5	9.28
A10	270	19.05	1.6	292	116	2425	20.9	25	104	3.2	6.36
A11	270	19.05	1.6	292	116	2500	21.6	25	104	3.2	6.19
A12	150	19.05	1.6	162	374	2900	7.8	15	63	3.2	7.16
A13	230	19.05	1.6	249	159	2525	15.9	22	90	3.2	6.44
A14	230	19.05	1.6	249	159	2700	17.0	22	90	3.2	6.56
A15	110	19.05	1.6	119	696	3400	4.9	12	50	3.2	9.85
A16	110	19.05	1.6	119	696	2900	4.2	12	50	3.2	8.24
A17	190	19.05	1.6	206	233	2700	11.6	19	77	3.2	7.87
A18	190	19.05	1.6	206	233	3000	12.9	19	77	3.2	7.81

response. After studying[14] the applicability of different criteria for "dynamic buckling", it is defined in the present investigation to occur in the transition between these two regions. This definition correlates with a dynamic buckling criterion proposed by Budiansky and Hutchinson[15], and it was used for determination of the dynamic buckling strain (ϵ_{cr_d}) of each column. Bending-compression plots for all the specimens are presented in[12]. A "Dynamic Load (Amplification) Factor" (DLF) is defined here by the ratio

$$\text{DLF} = \frac{\epsilon_{cr_d}}{\epsilon_{cr_E}} \tag{2.3}$$

and is presented in the tables for each column.

Results of tests on composite material (glass-epoxy) specimens are presented in Table 3. Experiments were also carried out for impact through an intermediary. A mass ($M_0 = 70$ gr) was attached to the upper edge of the column tested and the impulse was transfered from the striking mass to the specimen through the intermediate mass. This increases the duration of impulse. Results are shown in Table 4.

Discussion of test results

For the specimens tested DLF's of up to 30.6 were observed. Since the static buckling strains (ϵ_{cr_E}) assume ideally clamped perfect columns the real Dynamic Load Factors are larger. In Fig. 4 a logarithmic plot of DLF vs slenderness ratio (λ_{eff}) is presented. Since the results for steel and aluminum alloy columns are within the same experimental scatter it may be concluded that material properties do not significantly affect the dynamic buckling behavior. This conclusion is reinforced by the results of the glass-epoxy specimens. These composite columns have different material properties in the axial direction and the properties differ also from those of the metal specimens. For example, the longitudinal wave propagation velocity, which is approximately $c \approx 5000$ m/sec for steel and aluminum, ranges between $c \approx 3100$–3900 m/sec in the composite columns. The conclusion that materials properties do not significantly influence the dynamic buckling phenomenon is similar to that well known for static buckling of columns.

It seems reasonable that buckling strains depend upon conditions of loading. This was examined by comparison with the impact tests through an intermediate mass where longer durations of impulse were obtained. The results, presented in Fig. 6, show that smaller buckling strains are obtained for longer durations of impulse. This duration is expressed in a non-dimensional form by

$$\tau = \frac{cT}{2L} \tag{2.4}$$

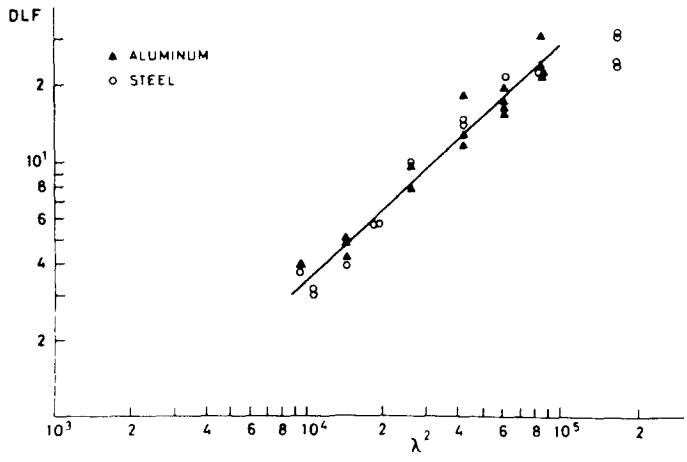

Fig. 4. "Dynamic Load (Amplification) Factor" vs slenderness for metal columns under impact.

Table 3. Clamped composite (glass/epoxy) columns under direct axial impact

Specimen No.	L Length [mm]	b Width [mm]	h Thickness [mm]	r Radius of gyration [mm]	λ_{eff} Effective slenderness	ϵ_{Cr_E} Euler buckling strain [μstrain]	ϵ_{Cr_n} Dynamic buckling strain [μstrain]	DLF Dynamic load factor	m Mass [gr]	M Striking mass [gr]	$\frac{\pi}{2}\sqrt{\frac{M}{m}}$	c Wave propagation velocity [m/sec]
1	2	3	4	5	6	7	8	9	10	11	12	13
ORT-00	75	19	1.6	0.49	77	1665	4075	2.45	8	77	4.9	3630
(ORT-00)							3075	1.85		77	4.9	
ORT-01	70	20	1.6	0.49	71	1958	4700	2.40	7	77	5.2	
ORT-10	73	18.5	1.6	0.49	74	1802	2850	1.58	7.5	77	5.0	3880
(ORT-10)							2475	1.37		77	5.0	
ORT-20	73	19	1.6	0.49	74	1802	2675	1.48	7.5	77	5.0	3620
ORT-30	72	19	1.6	0.48	75	1755	4400	2.51	7.5	77	5.0	3420
ORT-40	73	18.5	1.6	0.47	78	1622	3650	2.25	7.5	77	5.0	3160
0-00-12	120	18.5	1.5	0.46	130	584	2200	3.77	8	175	6.9	
0-00-14	140	18.5	1.5	0.46	152	427	2000	4.68	10.5	175	6.4	
0-00-18	180	18.5	1.6	0.49	184	292	2600	8.90	13	175	5.8	
0-40-09	90	18.5	1.5	0.44	102	949	2150	2.27	7	175	7.9	
0-40-15	150	18.5	1.4	0.41	183	295	2850	9.66	10.5	175	6.4	
0-40-25	250	18.5	1.4	0.41	305	106	1500	14.2	16	175	5.2	
0-50-22	220	18.5	1.4	0.40	275	131	1850	14.1	14	175	5.6	
0-65-10	100	18.5	1.5	0.41	122	663	2650	4.00	8	175	7.3	

Table 4. Clamped steel columns under axial impact through an intermediary ($M_0 = 70$ gr)

	L	b	h	λ_{eff}	ϵ_{Cr_E}	ϵ_{Cr_d}	DLF		m	M	V_{CT}
Specimen No.	Length [mm]	Width [mm]	Thickness [mm]	Effective slenderness	Euler buckling strain [μstrain]	Dynamic buckling strain [μstrain]	Dynamic load factor	Mass [gr]	Striking mass [gr]	$\frac{\pi}{2}\sqrt{\frac{M+M_0}{m}}$	Critical striking [m/sec]
1	2	3	4	5	6	7	8	9	10	11	12
T1	210	19.05	1.6	227	192	1650	8.6	55	275	3.9	5.27
T2	250	19.05	1.6	271	134	1850	13.8	64	275	3.6	5.90
T3	230	19.05	1.6	249	159	1725	10.8	60	275	3.8	6.01
T4	190	19.05	1.6	206	233	1625	7.0	50	275	4.1	~4.5
T5	170	19.05	1.6	184	292	2150	7.4	45.5	275	4.3	6.33
T6	140	19.05	1.6	152	427	2300	5.4	38	275	4.7	6.18
T7	110	19.05	1.6	119	697	2200	3.2	31	275	5.2	4.63

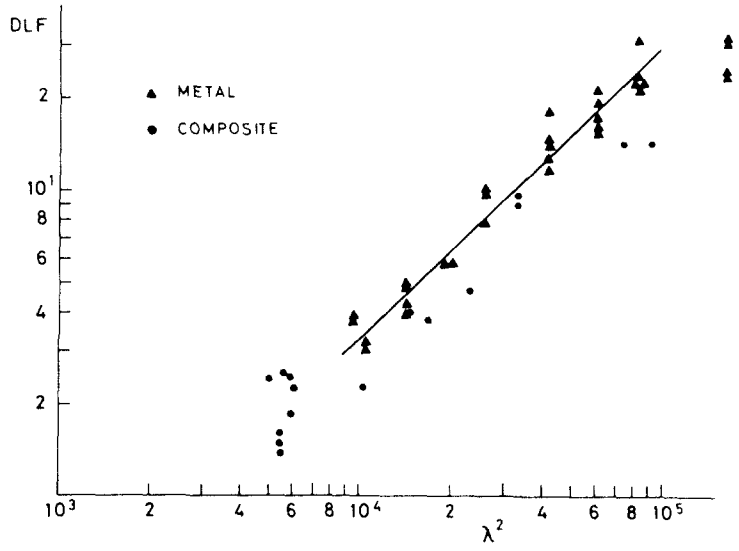

Fig. 5. "Dynamic Load (Amplification) Factor" vs slenderness for columns under direct impact.

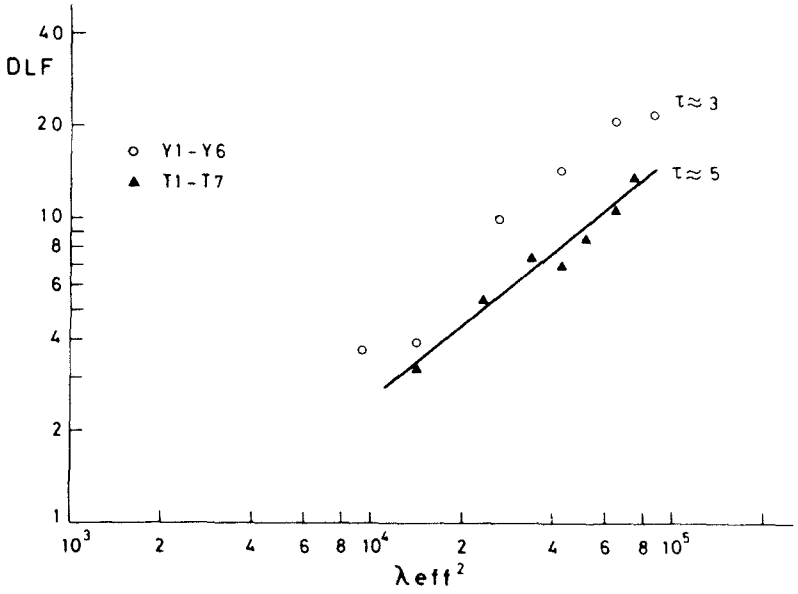

Fig. 6. Effect of longer impulse duration on D.L.F.

where T is the dimensional duration of compressive contact between the specimen and the striking mass. Assuming that static loading is represented by $\tau \to \infty$ one can conjecture that static buckling strain is a lower bound for dynamic buckling strains. The smaller the magnitude of τ the larger the DLF.

According to the definition of dynamic buckling employed in the experiments, the columns tested buckled elastically when permanent deformations were not yet observed. However, after occurrence of elastic buckling impact tests were continued with increasing striking velocities until plastic buckling waves were formed. These buckling patterns are presented in Fig. 7. It should be pointed out that this does not mean that elastic buckling waves have the same shapes.

The test results are discussed in more detail in[12], where also the relations between striking momentum and the resulting strain and impulse are considered.

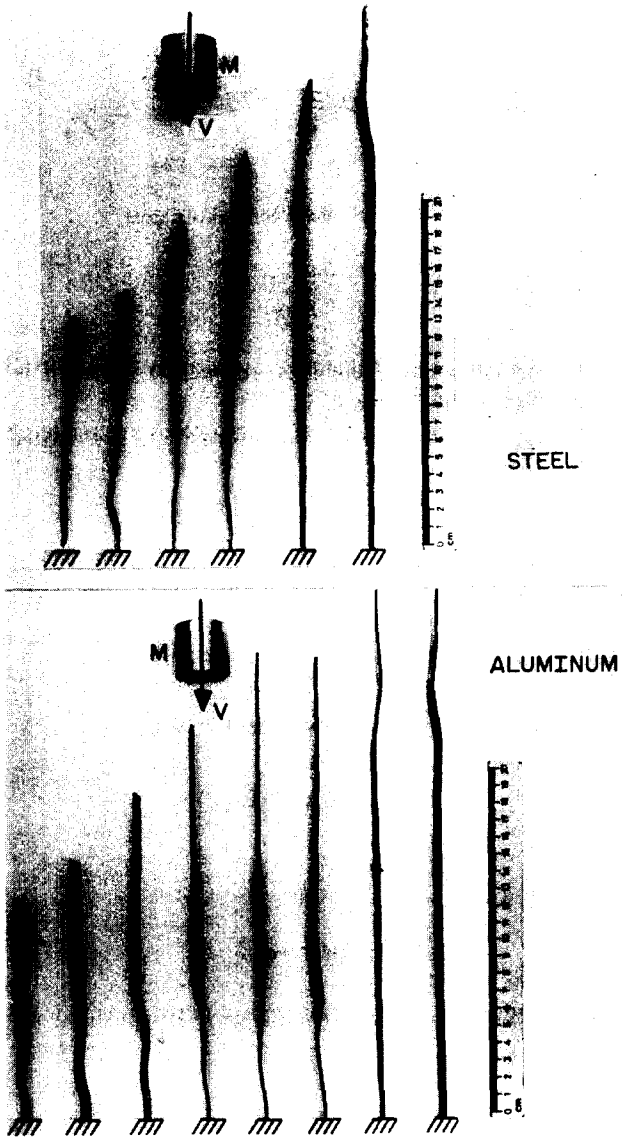

Fig. 7. Plastic buckling patterns of metal columns.

3. THEORY

A typical thin-walled beam is shown in Fig. 8. The usual Bernoulli–Navier hypothesis, that straight lines normal to the reference curve $\zeta = 0$ remain straight and normal during deformation, and small rotations are assumed, yielding equations of motion:

$$N_{x,x} = \rho h u_{,tt} \tag{3.1}$$

and

$$(M_{x,x} + N_x w_{,x} + \frac{1}{12}\rho h^3 w_{,xtt})_{,x} = \rho h w_{,tt} \tag{3.2}$$

where the force N_x and moment M_x per unit width are

$$(N_x, M_x) = \int_{-h/2}^{h/2} \sigma_x(1, z)\, dz \tag{3.3}$$

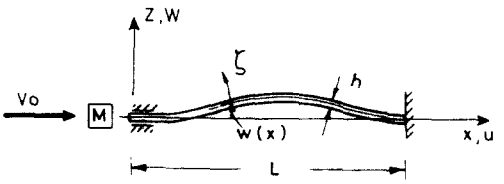

Fig. 8. Clamped column under axial impact.

u and w are the axial and lateral displacements, respectively, and ρ is the constant mass density of the column of uniform thickness h.

For the linear Hooke-type material, forces and deformations are related by

$$\begin{bmatrix} N_x \\ M_x \end{bmatrix} = \begin{bmatrix} A & B \\ B & D \end{bmatrix} \begin{bmatrix} \epsilon_x \\ \kappa_x \end{bmatrix} \tag{3.4}$$

where the elastic coefficients A, B and D are defined by

$$(A, B, D) = \int_{-h/2}^{h/2} (1, z, z^2) E(z)\, dz. \tag{3.5}$$

With eqns (3.4)–(3.5) and the deformation-displacement relations

$$\epsilon_x = u_{,x} + \frac{1}{2}(w^2_{,x} - w^2_{0,x}). \tag{3.6}$$

and

$$\kappa_x = -(w - w_0)_{,xx} \tag{3.7}$$

where $w(x, t) - w_0(x)$ is the deflection from the initial geometrical shape $w_0(x)$, the equations of motion (3.1) and (3.2) become:

$$A(u_{,xx} + w_{,x}w_{,xx} - w_{0,x}w_{0,xx}) - B(w - w_0)_{,xxx} = \rho h u_{,tt} \tag{3.8}$$

$$A\left[(u_{,x}w_{,x})_{,x} + \frac{3}{2} w^2_{,x} w_{,xx} - w_{0,x}\left(w_{0,xx}\, w_{,x} - \frac{1}{2} w_{0,x} w_{,xx}\right)\right] +$$

$$+ B[u_{,xx} + w_{0,xx}(w - w_0)_{,x}]_{,x} - D(w - w_0)_{,xxxx} = \rho h\left(w - \frac{h^2}{12} w_{,xx}\right)_{,tt}. \tag{3.9}$$

Introducing the longitudinal wave propagation velocity

$$c = \sqrt{\frac{A}{\rho h}} \tag{3.10}$$

the "symmetric" radius of gyration of the cross-section

$$r_0 = \sqrt{\frac{D}{A}} \tag{3.11}$$

and the corresponding slenderness ratio

$$\lambda_0 = \frac{L}{r_0} \tag{3.12}$$

eqns (3.8) and (3.9) can be rewritten in non-dimensional form as

$$\bar{u}'' + \bar{w}'\bar{w}'' - \bar{w}_0'\bar{w}_0'' - \frac{B}{AL}(\bar{w} - \bar{w}_0)''' = \ddot{\bar{u}} \tag{3.13}$$

$$(\bar{u}'\bar{w}')' + \frac{3}{2}\bar{w}'2\bar{w}'' - \bar{w}_0'(\bar{w}_0''\bar{w}' - \frac{1}{2}\bar{w}_0'\bar{w}'') + \frac{B}{AL}[\bar{u}'' + \bar{w}_0''(\bar{w} - \bar{w}_0)']'$$

$$-\frac{1}{\lambda_0^2}(\bar{w} - \bar{w}_0)'''' = \ddot{\bar{w}} - \frac{1}{12}\left(\frac{h}{L}\right)^2 \ddot{\bar{w}}'' \tag{3.14}$$

with the non-dimensional displacements

$$\bar{u} = \frac{u}{L}\ ,\ \bar{w} = \frac{w}{L}\ . \tag{3.15}$$

Prime ( )' and dot $(\cdot)$ represent derivatives with respect to the non-dimensional axial coordinate $\bar{x} = x/L$ and time $\bar{t} = ct/L$, respectively.

Dynamics of striking mass

At the initiation of contact between the striking mass (M) and the edge $x = 0$ of the column, the axial displacement of the mass is defined

$$U(t = 0) = 0 \tag{3.16}$$

and the striking velocity is

$$V(t = 0) = U_{,t}(t = 0) = V_0. \tag{3.17}$$

This mass is decelerated by the repulsive force $bN_x(x = 0)$ at the impacted edge and therefore

$$V(t) = V_0 + \frac{b}{M}\int_0^t N_x(x = 0)\,\mathrm{d}t \tag{3.18}$$

and

$$U(t) = \int_0^t V(t)\,\mathrm{d}t. \tag{3.19}$$

In non-dimensional formulation

$$\bar{V}(\bar{t}) = \bar{V}_0 + \frac{m}{M}\int_0^{\bar{t}} \epsilon_x(x = 0)\,\mathrm{d}\bar{t} \tag{3.20}$$

where m is the mass of the column and

$$\bar{V} = \frac{V}{c}\ ,\ \bar{V}_0 = \frac{V_0}{c}\ ,\ \bar{t} = \frac{ct}{L}\ . \tag{3.21}$$

Initial and boundary conditions

At the instant of initiation of collision the column is at rest, and only the edge $x = 0$ is perturbed. Assuming a rigid striking mass, the initial conditions are:

$$w(t = o) = w_0$$

$$w_{,t}(t = 0) = u(t = 0) = u_{,t}(x > 0, t = 0) = 0 \tag{3.22}$$

$$u_{,t}(x = 0, t = 0) = V_0.$$

The boundary conditions are those for a clamped column:

$$w = w_{,x} = 0 \quad x = 0, L \tag{3.23}$$

and the edge $x = L$ is fixed:

$$u(x = L) = 0. \tag{3.24}$$

At the impacted edge

$$u(x = 0) = U \text{ when } N_x(x = 0) < 0 \tag{3.25}$$

otherwise

$$N_x(x = 0) = 0.$$

The last condition is time-dependent. It expresses the mutual ineraction between the motions of the specimen and the striking mass. Simultaneous solution is therefore required for both bodies.

Finite difference approach

The differential equations of motion were approximated by a finite difference approach using central difference formulae. A detailed description of the process is presented in [13]. The equations of motion of the column then become:

$$u(x, t + \Delta t) = u(x, t) + R_L\Big\{u(x, t) - u(x, t - \Delta t) + \frac{(\Delta t)^2}{\rho h}[A(u_{,xx} + w_{,x}w_{,xx} - w_{0,x}w_{0,xx}) - B(w - w_0)_{,xxx}]\Big\} \tag{3.26}$$

and

$$w(x, t + \Delta t) - \frac{h^2}{12}w_{,xx}(x, t + \Delta t) = w(x, t) - \frac{h^2}{12}w_{,xx}(x, t) + R_T\Big\{w(x, t) - w(x, t - \Delta t) - \frac{h^2}{12}[w_{,xx}(x, t) - w_{,xx}(x, t - \Delta t)] + \frac{(\Delta t)^2}{\rho h}\Big\{A\Big[u_{,x}w_{,x})_{,x} + \frac{3}{2}w_{,x}^2 w_{,xx} - w_{0,x}\Big(w_{0,xx}w_{,x} - \frac{1}{2}w_{0,x}w_{,xx}\Big)\Big] + B[u_{,xx} + w_{0,xx}(w - w_0)_{,x}]_{,x} - D(w - w_0)_{,xxx}\Big\}\Big\}. \tag{3.27}$$

These equations contain damping terms

$$R_L = \exp(-C_L\Delta t), \quad R_T = \exp(-C_T\Delta t) \tag{3.28}$$

for the longitudinal and transverse motions, respectively.

The displacement of the striking mass varies during the first time interval Δt from zero to

$$U(t = \Delta t) = V_0\Delta t\Big[1 - \frac{\Delta t}{2}\frac{b\sqrt{(A\rho h)}}{M}\Big] \tag{3.29}$$

and later, when $t \geq 2\Delta t$, to

$$U(t + \Delta t) = 2U(t) - U(t - \Delta t) + \frac{Ab(\Delta t)^2}{M\Delta x}[u(\Delta x, t) - u(0, t)]. \tag{3.30}$$

The last equation is valid only if the stress wave had already passed the first mesh distance Δx. Before that

$$U=(t+\Delta t)=U(t)\left[2-\frac{(\Delta t)^2}{t}\frac{b\sqrt{(A\rho h)}}{M}\right]-U(t-\Delta t) \tag{3.30.1}$$

is the proper equation.

A computer program, IMPCOL, which solves the finite difference equations of the problem is described in[13], together with convergence tests for the numerical solution. It was found there that $\Delta x \gtrsim \frac{L}{16}$ yields satisfactory results. Theoretical considerations show that for slender columns, where $\Delta x > 2r$ (r is the radius of gyration of the cross-section) is commonly used,

$$c\Delta t \leq \Delta x \tag{3.31}$$

is the condition for convergence and stability of the solution. It was shown numerically in [13], that for more accurate results Δt should be chosen to satisfy the equality $c\Delta t = \Delta x$. This may be explained by the fact that the time interval $\Delta t < \Delta x/c$ is too short for a disturbance to propagate between two adjacent spatial mesh points. Hence, the finite-difference formulation is an appropriate representation of the physical phenomenon only when $c\Delta t = \Delta x$. Otherwise a discretization error is propagated.

Comparison with experiments

A steel column was bent and the initial geometrical shape was measured and presented in[13]. This shape approximates that of the clamped–clamped buckling mode. The amplitude of the measured imperfection was $w_{0_{max}} = 1.1\,h = 1.76$ mm. The column was impacted by a mass $M = 0.175$ kg ($\tau \approx 2.6$), with gradually increasing striking velocities until buckling occurred. A simulation of this experiment was solved numerically and the results are compared.

First, the compressive strains in the middle of the column length are compared in Figs. 9(a) and (b). One can note the good agreement. A detailed discussion of the comparison is presented in[13].

The most interesting comparison is between the flexure-compression curves, since these curves yield the dynamic buckling strain. The growth of the maximum deflection is shown in Fig. 10 vs the axial compressive strain for two columns: the measured one ($w_{0_{max}} = 1.76$ mm) and for a column with an "amplified" imperfection ($w_{0_{max}} = 2.36$ mm) of the same shape. The latter represents the effective imperfection, which includes, in addition to the geometrical

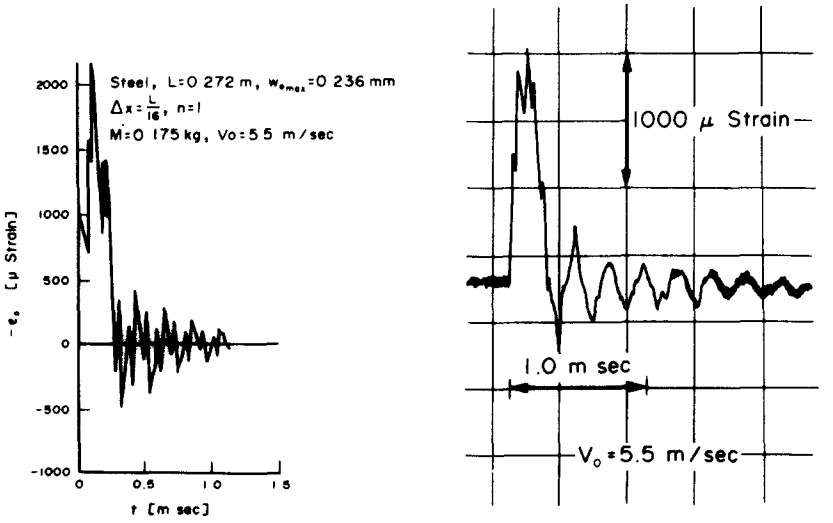

Fig. 9. Comparison of experimental and theoretical compressive strains.

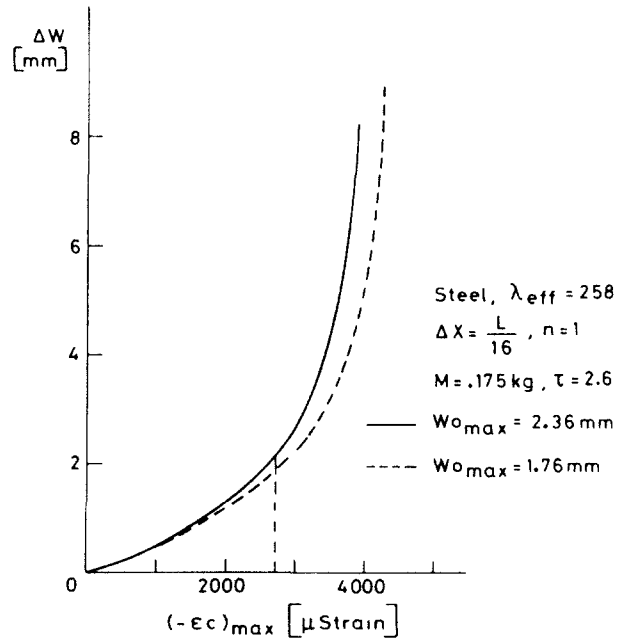

Fig. 10. Maximum deflection vs maximum axial strain.

imperfection of the column, the equivalent imperfections due to loading alignment, material, etc. It was found[13] that an imperfection of about 0.6 mm amplitude should be added to the specimens tested to approximately represent the effective imperfection in the present test rig.

The slope of the curve in Fig. 10 is presented in Fig. 11 vs the axial strain. This curve is useful for determination of the dynamic buckling load according to the Budiansky–Hutchinson type criterion[15]. The dynamic buckling strain predicted from Fig. 11, $(-\epsilon_c)_{max_{cr}} \approx 2700\mu$-strain, is in good agreement with the experimental result presented in Fig. 12 ($\sim 2400\mu$-strain). It should be noted that the results for this column are not presented in the tables, since the column has a much higher level of imperfection than the other columns not bent intentionally, and can therefore not be compared.

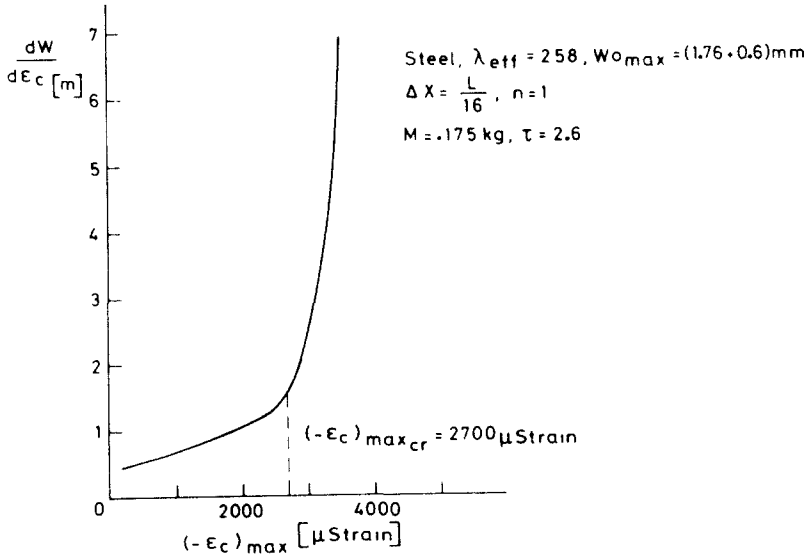

Fig. 11. Slope dw/dε vs maximum axial strain.

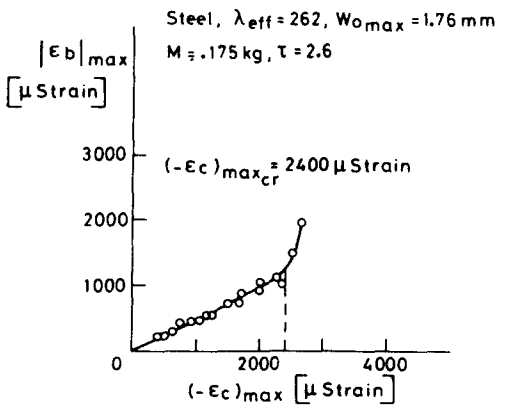

Fig. 12. Experimental bending response vs maximum axial compression.

Other examples of comparisons between theoretical and experimental results are presented in Figs. 13 and 14. The dashed lines represent dynamic buckling strains of the columns tested, and good agreement with the computed behavior is observed.

Effect of imperfection

A perfectly straight ($w_0 = 0$) and symmetric ($B = 0$) column does not buckle under an axial impulsive compression. Real columns, however, are always imperfect and their dynamic buckling loads are dependent on the shape and the magnitude of their initial imperfection. It can be seen in Fig. 15 that the amplitude of w_0 is the primary factor determining the dynamic buckling strain, the number of waves is also very significant, while the location of the peak does not influence the flexture-compression behavior of the column. The behavior of a column with as assumed initial imperfection of the shape

$$w_0(x) = w_0 \cdot \frac{1}{2}\left(1 - \cos\frac{\pi x}{L_{eff}}\right) \tag{3.32}$$

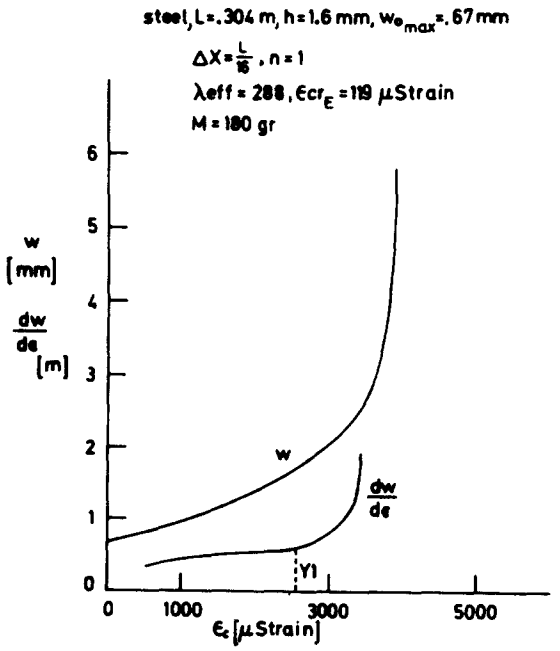

Fig. 13. Numerical evaluation of buckling of column Y1.

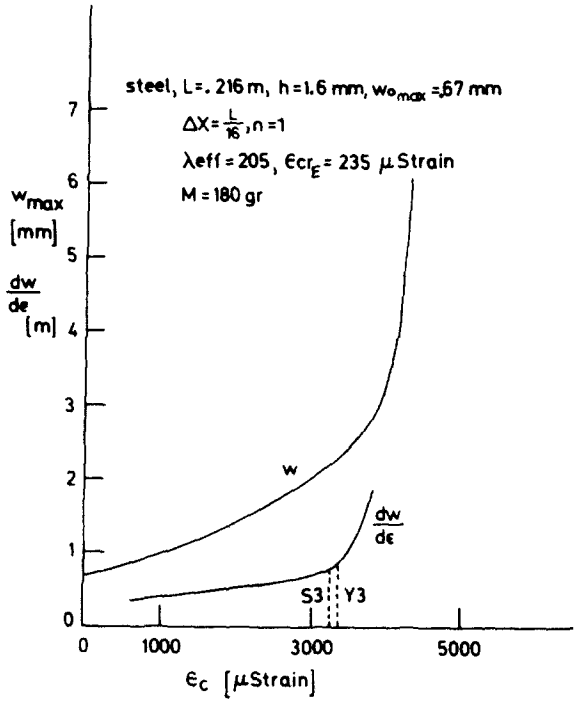

Fig. 14. Numerical evaluation of buckling of columns Y3 and S3.

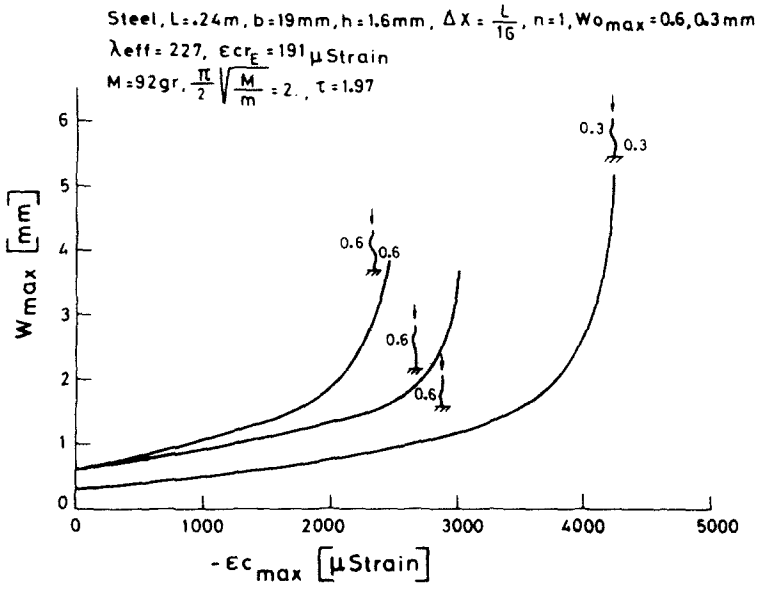

Fig. 15. Effect of initial geometrical imperfection on buckling strain.

was tested numerically for various magnitudes of the amplitude w_0. The results are presented in Fig. 16, and it is obvious that the larger the initial imperfection, the smaller the maximum axial strain. This behavior is entirely different from that of static buckling of columns where the upper bound of the axial load is independent of the magnitude of the initial imperfection.

The curves of Fig. 16 can be represented fairly closely by the function

$$\frac{w}{w_o} = 1 + \alpha\epsilon + \frac{\beta\epsilon}{\epsilon_{cr}(\epsilon_{cr} - \epsilon)} \tag{3.33}$$

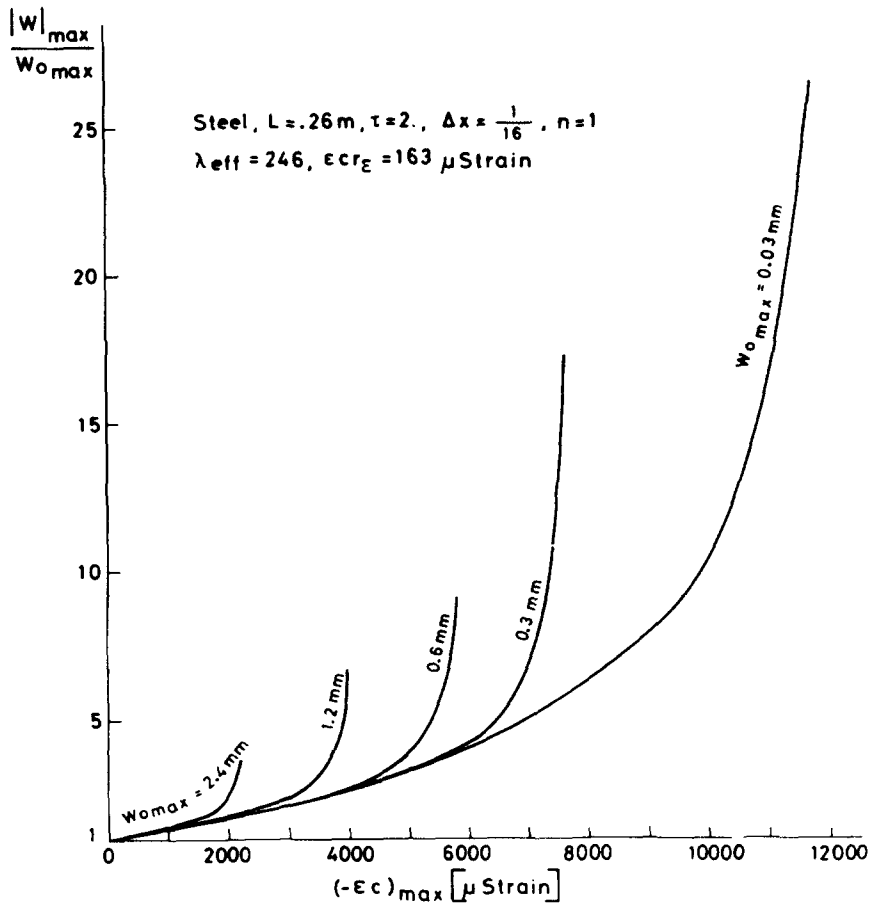

Fig. 16. Nondimensional dynamic deflection-compression plots for various magnitudes of initial geometrical imperfection.

where α is a constant common to all the curves, whereas β and ϵ_{cr} are constants that differ for each w_0 curve. A simple manipulation of eqn (3.33) yields the following equation:

$$\frac{w - w_0}{\epsilon} = \frac{\Delta w}{\epsilon} = w_0\left(\alpha + \frac{\beta}{\epsilon_{cr}^2}\right) + \frac{1}{\epsilon_{cr}}(\Delta w - \alpha w_0 \epsilon). \tag{3.34}$$

when one sets $\alpha = 0$ and $\beta = \epsilon_{cr}$ in the last equation, it reduces to

$$\frac{\Delta w}{\epsilon} = \frac{1}{\epsilon_{cr}}(w_0 + \Delta w) \tag{3.34.1}$$

which is the well-known equation of the Southwell plot. Hence, eqn (3.34) may be called a "generalized Southwell equation". A plot of $\Delta w/\epsilon$ vs $\Delta w - \alpha w_0 \epsilon$ provides ϵ_{cr}, which is the reciprocal value of the slope of the line. Unfortunately, the dynamic Southwell plot requires a previous knowledge of the term Δw_0—a requirement which does not exist in the case of static buckling. However, when $\alpha w_0 \epsilon$ is much smaller than Δw this limitation vanishes. Since ϵ is bounded by ϵ_{cr} while Δw is unbounded, there is always a region where the condition $\alpha w_0 \epsilon \ll \Delta w$ is fulfilled. Therefore a plot of $\Delta w/\epsilon$ vs Δw (the dots in Fig. 17) is a sufficiently close approximation of the exact dynamic plot which is represented by the straight line in Fig. 17.

RESULTS AND DISCUSSION

The major disadvantage of the upper bound ϵ_{cr} is that, since it is associated with an infinite deflection, it can never be reached. This is true, however, for either static or dynamic buckling

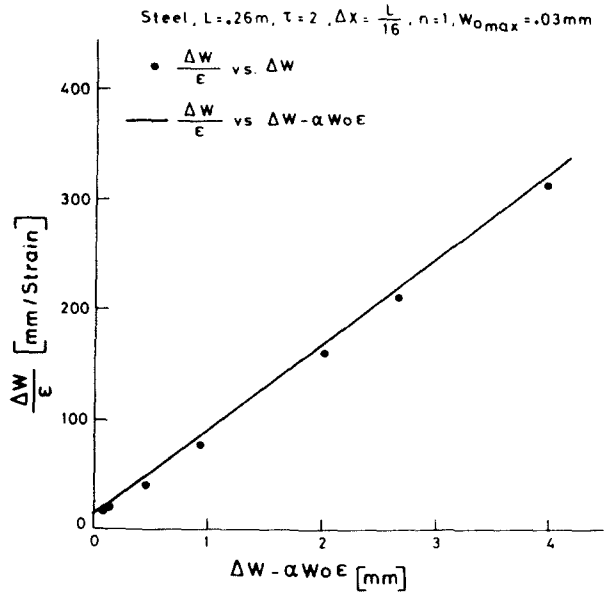

Fig. 17. Dynamic Southwell plot.

of a column, and the Dynamic Load Amplification Factor, which may be defined here by the ratio of the dynamic to static upper bounds of the axial strain

$$\mathrm{DLF} = \frac{\epsilon_{cr}}{\epsilon_{cr_E}} \tag{3.35}$$

represents therefore a real amplification. The definition of eqn (3.35) yields DLF's which are larger than those obtained by eqn (2.3). However, since comparisons with experimental results were already presented, the upper bound criterion is adopted here for phenomenological studies.

From the experimental results it was concluded that the magnitude of the dynamic buckling load of a column under axial impulse of a certain duration is determined by its slenderness ratio. This conclusion is confirmed here by Fig. 18. It appears that for more slender columns, the static buckling strain ($\tau \to \infty$) decreases rapidly compared with the moderate decrease of dynamic buckling strains. This means that large DLF's are obtained for more slender columns, as can be seen in Fig. 19.

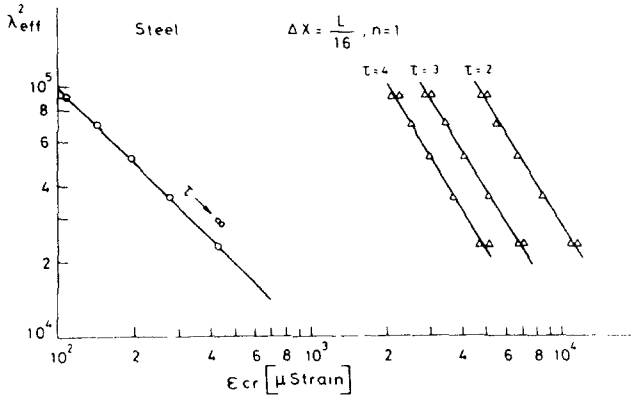

Fig. 18. Critical strain vs slenderness for steel columns.

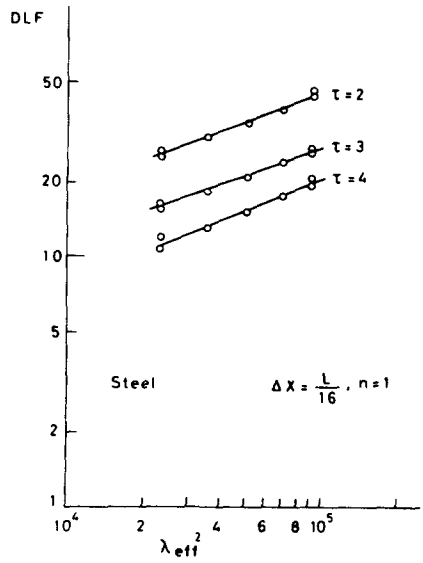

Fig. 19. D.L.F. vs slenderness for steel columns.

The last figures show also the effect of the duration of impulse. The longer the duration of the axial impulse, the smaller the load sustained by a certain column. But even for the longest duration of impulse ($\tau \to \infty$), ϵ_{cr} is never less than the static critical strain ϵ_{cr_E}. The validity of this statement was verified up to $\tau = 160$ (see Fig. 20) where a steel column of $m = 47$ gr is impacted by a huge striking mass $M = 492$ kg and very low striking velocities (gravitational effects are not included). The axial strains exceed ϵ_{cr_E}, as presented in Fig. 20. It is therefore concluded that the Dynamic Load Amplification Factor is always greater than unity, and as $\tau \to \infty$, DLF$\to$1.

Columns made from different materials have the same Euler buckling strain, if their effective slenderness is identical. In dynamic problems, however, where inertia effects must be considered, different materials, with different mass densities, may be expected to yield different buckling strains. A comparison of results for several materials is therefore presented in Fig. 21. Slight differences may be noticed for the different materials, but they are small and insignificant. From this result, together with the experimental observations, one may conclude

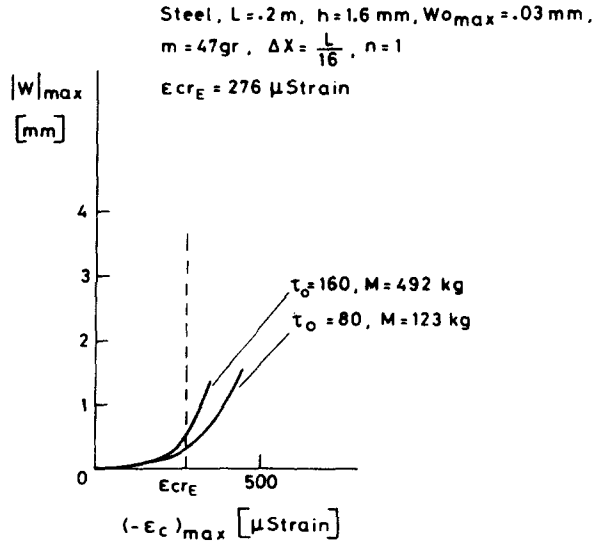

Fig. 20. Column response for large impulse durations.

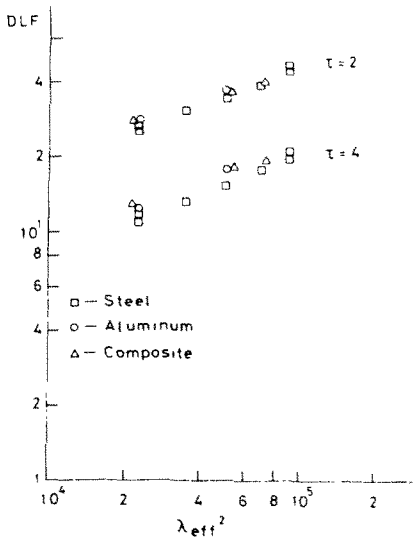

Fig. 21. D.L.F. vs slenderness for columns of various materials.

that material properties, like flexural rigidity, wave propagation velocity and density, have only secondary effects on the dynamic buckling of columns. It should be mentioned that mechanical damping coefficients were varied only by ± 10%, and these variations did not influence the dynamic buckling behavior. It is, however, possible that larger variations of C_L and C_T in eqns (3.28) would affect the buckling strains more significantly.

4. CONCLUSIONS

The response and buckling of columns under axial impact were studied experimentally and theoretically. The analytical solution, by a finite-difference approximation of the differential equations of motion, correlates well with test results. It was found that good results are obtained by dividing the length of the column into only 16 elements Δx. A choice of time increment Δt which corresponds to a propagation of axial stress wave along a single mesh distance Δx yields the best results.

A relation was proposed between the applied axial strain and the resulting deflection of the impacted column. This relation provides a "dynamic Southwell equation" and a "generalized Southwell plot" for prediction of critical axial strain. One should note that here purely elastic material behavior is assumed to prevail even for large deflections.

In the experimental studies another criterion was employed that permits determination of the dynamic buckling load before large deflections occur.

Dynamic buckling strains are strongly dependent upon initial geometrical imperfections, duration of impulse and slenderness of the column. Longer durations of impulsive loading or larger magnitudes of initial geometrical imperfection considerably decrease the dynamic buckling strain. Yet, the dynamic critical strain is never less than the static one. A "Dynamic Load (Amplification) Factor" (DLF) was defined. Results were then presented as linear plots of DLF vs slenderness ratio on a logarithmic scale. The larger the slenderness, the larger the DLF. Material properties (except mechanical damping) were found to have only secondary effects on the dynamic buckling strain.

Acknowledgements—The authors wish to thank Mr. S. Nachmani and Mr. A. Grunwald of the staff of the Aeronautical Structures Laboratory for their assistance with the experiments, and Mr. A. Neer for useful discussions. They also wish to thank Mrs. D. Mirkin for the typing of the manuscript and Mrs. I. Nitzan for the preparation of the figures.

REFERENCES

1. V. C. Koning and J. Taub, Impact buckling of thin bars in the elastic range hinged at both ends. *Luftfahrtforschung* **10**(2), 55 (1933).
2. J. H. Meier, On the dynamics of elastic buckling. *J. Aeronaut. Sci.* **12**, 433–440 (1945).

3. J. F. Davidson, Buckling of struts under dynamic loading. *J. Mech. Phys. of Solids* **2**, 54–66 (1953).
4. N. J. Hoff, The dynamics of the buckling of elastic columns. *J. Appl. Mech.* **17**(1), 68–74 *Trans. ASME* (1953).
5. N. J. Hoff, S. V. Nardo and B. Erickson, The maximum load supported by an elastic column in a rapid compression test. *Proc. 1st U.S. Nat. Cong. Appl. Mech.* pp. 419–423. Chicago (1951).
6. B. Erickson, S. V. Nardo, S. A. Patel and N. J. Hoff, An experimental investigation of the maximum loads supported by elastic columns in rapid compression tests. *Proc Soc. of Experim. Stress Anal.* **14**(1), 13–20 (1956).
7. B. Hegglin, Dynamic buckling of columns. *SUDAER Rep. No.* 129, Stanford University, Stanford, California (1962).
8. E. Sevin, On the elastic bending of columns due to dynamic axial forces including effects of axial inertia. *J. Appl. Mech.* **27**(1), 125–131. *Trans. ASME* (1960).
9. W. Goldsmith, *Impact*. Edward Arnold, London (1960).
10. T. Hayashi and Y. Sano, Dynamic buckling of elastic bars, 1st report, The case of low velocity impact. *Bull. JSME* **15**(88), 1167–1175 (1972).
11. T. Hayashi and Y. Sano, Dynamic buckling of elastic bars, 2nd report, The case of high velocity impact. *Bull. JSME* **15**(88), 1176–1184 (1972).
12. J. Ari-Gur, T. Weller and J. Singer, Experimental studies of columns under axial impact. *TAE Rep. No.* 346, Dept. of Aeronautical Engineering, Technion-Israel Institute of Technology, Haifa, Israel (1978).
13. J. Ari-Gur, T. Weller and J. Singer, Theoretical studies of columns under axial impact and experimental verification. *TAE Rep. No.* 377, Dept. of Aeronautical Engineering, Technion-Israel Institute of Technology, Haifa, Israel (1979).
14. J. Singer, T. Weller, A. Lebai and J. Ari-Gur, Preliminary dynamic stability studies using vibraion techniques for definition of boundaries. *Rep. ASL-95*, Dept. of Aeronautical Engineering, Technion-Israel Institute of Technology, Haifa, Israel (1978).
15. B. Budiansky and J. W. Hutchinson, Dynamic buckling of imperfection sensitive structures. *Prox. 11th Int. Cong. Appl. Mech.* Munich, 1964, (Edited by H. Görtler), pp. 636–651. Springer-Verlag, Berlin (1966).